Forward modeling of seismic-while-drilling data in anisotropic viscoelastic media with anisotropic attenuation

Ali Fathalian, Nasser Kazemi, Jean Auriol, Daniel O Trad, Kristopher A Innanen, Roman Shor

2022 EAGE ANNUAL
83RD CONFERENCE & EXHIBITION
MADRID | SPAIN

Forward modeling of seismic-while-drilling data in anisotropic viscoelastic media with anisotropic attenuation

Ali Fathalian, Nasser Kazemi, Jean Auriol, Daniel O. Trad, Kristopher A. Innanen, and Roman Shor

Summary

We have derived a system of equations for seismic-while-drilling viscoelastic wave modeling in a medium with transverse isotropy (TI) in velocity and attenuation based on a standard linear solid model. Considering anisotropy in attenuation changes the conventional frequency-dependent constant Q model to a Q matrix in a 2D problem. We derive and represent the new system of equations for this stress-strain relationship. The numerical implementation of this system is with the finite-difference method (second-order accuracy in time and fourth-order accuracy in space). Also, we use a drillstring dynamics modeling based on wave equation to model the source signature of seismic-while-drilling data. Our results show that the proposed approach is capable of capturing TI effects in attenuation and illustrating the efficiency of this system of equations for applications in seismic imaging and inversion.

Forward modeling of seismic-while-drilling data in anisotropic viscoelastic media with anisotropic attenuation

Introduction

Attenuation and anisotropy are increasingly indispensable components of wavefield simulation in seismic exploration and monitoring applications. They are essential in modern seismic amplitude modeling and reverse time migration (RTM) procedures. A constant-Q model proposed by Kjartansson (1979) enables us to perfectly describe the frequency-independent Q anelastic behavior by using fewer parameters. This model has been used to represent the attenuation behavior in viscoacoustic wave equations (Fathalian et al., 2020, 2021) and viscoelastic wave equations (Zhu and Carcione, 2014). In this work, we extend the isotropic formulation to a general anisotropic viscoelastic wave equation, allowing us to model anisotropic attenuation. We derive the equations for a viscoelastic VTI medium with anisotropy in velocity and attenuation based on the standard linear solid model. When the quality factor goes to infinity, the equations reduce to the derived system of equations introduced by Duveneck and Bakker (2011) for TI anisotropic velocity.

Theory

The general stress-strain relationship in viscoelastic media reads (Christensen, 1982)

$$\sigma_{ij} = G_{ijkl} * \dot{\varepsilon}_{kl}, \tag{1}$$

where $*$ denotes convolution in time, σ_{ij} is the stress tensor, ε_{kl} is the strain tensor and G_{ijkl} is the stiffness tensor that determines the behavior of material. We will consider standard linear solid models (SLS) in anelastic anisotropic media. The time response for this model is given by (Blanch et al., 1993)

$$G_{ijkl}(t) = M^R_{ijkl}\left(1 - \frac{1}{L}\sum_{\ell=1}^{L}(1 - \frac{\tau_{\varepsilon\ell}}{\tau_{\sigma\ell}})e^{-\frac{t}{\tau_{\sigma\ell}}}\right)H(t), \tag{2}$$

where L is the number of mechanisms, M^R_{ijkl} is the relaxation modulus of the medium (Pipkin, 1986), and $H(t)$ is the heaviside function. The $G_{ijkl}(t)$ is equivalent to a series of L standard linear solids (Blanch et al., 1993), and is also the best Padé approximation for constant-Q (Day and Minster, 1984). Elements $\tau_{\sigma\ell}$ and $\tau_{\varepsilon\ell}$ refer to the stress and strain relaxation times of the ℓth mechanism. In Voigt notation (using the identification $G_{IJ} \leftrightarrow G_{ijkl}$ by mapping of indexes $1,2,3,4,5,6$ into the pairs $(1,1),(2,2),(3,3),(2,3),(1,3)$ $,(1,2)$) the components of the tensor of anelasticity become

$$G_{IJ}(t) = M^R_{IJ}\left(1 - \frac{1}{L}\sum_{\ell=1}^{L}(1 - \frac{\tau_{\varepsilon\ell}}{\tau_{\sigma\ell}})e^{-\frac{t}{\tau_{\sigma\ell}}}\right)H(t). \tag{3}$$

The anelasticity matrix for transversely isotropic media with vertical axis (VTI media) can be written as (Du et al., 2008)

$$G(t) = \begin{pmatrix} M_{11} & M_{12} & M_{13} & 0 & 0 & 0 \\ M_{12} & M_{22} & M_{23} & 0 & 0 & 0 \\ M13 & M_{23} & M_{33} & 0 & 0 & 0 \\ 0 & 0 & 0 & M_{44} & 0 & 0 \\ 0 & 0 & 0 & 0 & M_{55} & 0 \\ 0 & 0 & 0 & 0 & 0 & M_{66} \end{pmatrix}\left(1 - \frac{1}{L}\sum_{\ell=1}^{L}(1 - \frac{\tau^{\varepsilon\ell}_{ij}}{\tau^{\sigma\ell}})e^{-\frac{t}{\tau^{\sigma\ell}}}\right)H(t). \tag{4}$$

The viscoacoustic wave equation in VTI media can be obtained by a combination of equations 1 and 4. Hence, the relation between stress and strain is given by

$$\partial_t \sigma_{11} = M_{11}\left(\frac{\tau^{\varepsilon\ell}_{11}}{\tau^{\sigma\ell}}\right)\partial_x u_x + M^{13}\left(\frac{\tau^{\varepsilon\ell}_{13}}{\tau^{\sigma\ell}}\right)\partial_z u_z + r_{11}, \tag{5}$$

$$\partial_t \sigma_{33} = M_{13}\left(\frac{\tau_{13}^{\varepsilon\ell}}{\tau^{\sigma\ell}}\right)\partial_x u_x + M^{33}\left(\frac{\tau_{33}^{\varepsilon\ell}}{\tau^{\sigma\ell}}\right)\partial_z u_z + r_{33}, \tag{6}$$

$$\partial_t \sigma_{13} = M_{55}\left(\frac{\tau_{55}^{\varepsilon\ell}}{\tau^{\sigma\ell}}\right)(\partial_x u_x + \partial_z u_z) + r_{13}, \tag{7}$$

where $M_{11} = \rho V_P^2(1+2\varepsilon), M_{33} = \rho V_P^2, M_{55} = \rho V_S^2, (M_{13}+M_{55})^2 = \rho^2(V_P^2 - V_S^2)^2 + 2\delta\rho^2 V_P^2(V_P^2 - V_S^2)$, and $r_{ij} = M_{ij}\left(1 - \frac{1}{L}\sum_{\ell=1}^{L}\frac{1}{\tau^{\sigma\ell}}(1 - \frac{\tau_{ij}^{\varepsilon\ell}}{\tau^{\sigma\ell}})\right)H(t) * \partial_i u_j$.

Since one of the inputs of seismic wavefield simulation is the source signature, we briefly introduce our approach for estimating the source signature of the drillbit-rock interaction. Following the approach of Auriol et al. (2019) and Kazemi et al. (2020), we implement wave equation modeling of drillstring dynamics with topside and bit-rock boundary conditions combined with top-drive hook-load and hook-speed measurements to estimate the drill bit source signature. To do so, we start with wave equation modeling of axial motion in the drillstring

$$\frac{\partial^2 \mathbf{u}(\mathbf{x},t)}{\partial t^2} - c^2\frac{\partial^2 \mathbf{u}(\mathbf{x},t)}{\partial x^2} = -k\frac{\partial \mathbf{u}(\mathbf{x},t)}{\partial t}, \tag{8}$$

where $c = \sqrt{\frac{E}{\rho}}$ is the velocity of the drill pipe, E is the Young's module, ρ is the drill pipe density, k is the damping factor, and $\mathbf{u}(\mathbf{x},t)$ is the axial motion in the drillstring in time t and distance along drillstring $\mathbf{x}$. The axial force follows $\mathbf{w}(t,\mathbf{x}) = AE\frac{\partial \mathbf{u}(\mathbf{x},t)}{\partial x}$, and the axial velocity is $\mathbf{v}(t,\mathbf{x}) = \frac{\partial \mathbf{u}(\mathbf{x},t)}{\partial t}$. Then, the top-drive boundary condition can be written as

$$-EA\frac{\partial \mathbf{u}(\mathbf{x},t)}{\partial t} = \mathbf{w}(t,0), \tag{9}$$

where $\mathbf{w}(t,0)$ is the topside weight function, and A is the cross-sectional area of the drill pipe. Moreover, the drillbit-rock interaction follow

$$M_b\frac{\partial \mathbf{v}(t,L)}{\partial t} = -\mathbf{w}_b(\mathbf{v}(t,L),\mathbf{w}(t,L)) + \mathbf{w}(t,L), \tag{10}$$

where M_b is the mass of bottom hole assembly, $\mathbf{w}_b$ is the weight-on-bit, and L is the length of drillstring measured from the surface to the drillbit. Through a backstepping approach and by using top-drive measurements, equations (8)-(10) can be solved for the drill bit source signature

$$\begin{aligned} w(t,L) =& \frac{EA}{2c}(\mathrm{e}^{-\frac{kL}{2c}}v(t-\frac{L}{c},0) - \mathrm{e}^{\frac{kL}{2c}}v(t+\frac{L}{c},0)) + \frac{1}{2}(\mathrm{e}^{-\frac{kL}{2c}}w(t-\frac{L}{c},0) + \mathrm{e}^{\frac{kL}{2c}}w(t+\frac{L}{c},0)) \\ &+ \int_{-\frac{L}{c}}^{\frac{L}{c}}(f_u(s)+f_z(s))v(t-s,0)ds + \int_{-\frac{L}{c}}^{\frac{L}{c}}\frac{c}{EA}(f_u(s)-f_z(s))w(t-s,0)ds \end{aligned} \tag{11}$$

where f_z and f_u are functions that depend on drilling parameters (Auriol et al., 2019). Here, we only considered the axial motion of the drillstring and the rotational motion is ignored. Improvements to this approach are necessary to capture the full elastic nature of the drill bit source. Data driven estimation of the drill bit source signature introduced by Kazemi and Sacchi (2014) is another alternative that showed promise when applied to SWD data (Kazemi et al., 2018a).

Examples

To evaluate the performance of our forward modeling engine, we use the Sigsbee model. Figure 1a shows the primary velocity of the Sigsbee model. There is a strong salt body in the model, which deteriorates the wavefields and results in poor illumination of the sub-salt structure in the case of surface seismic

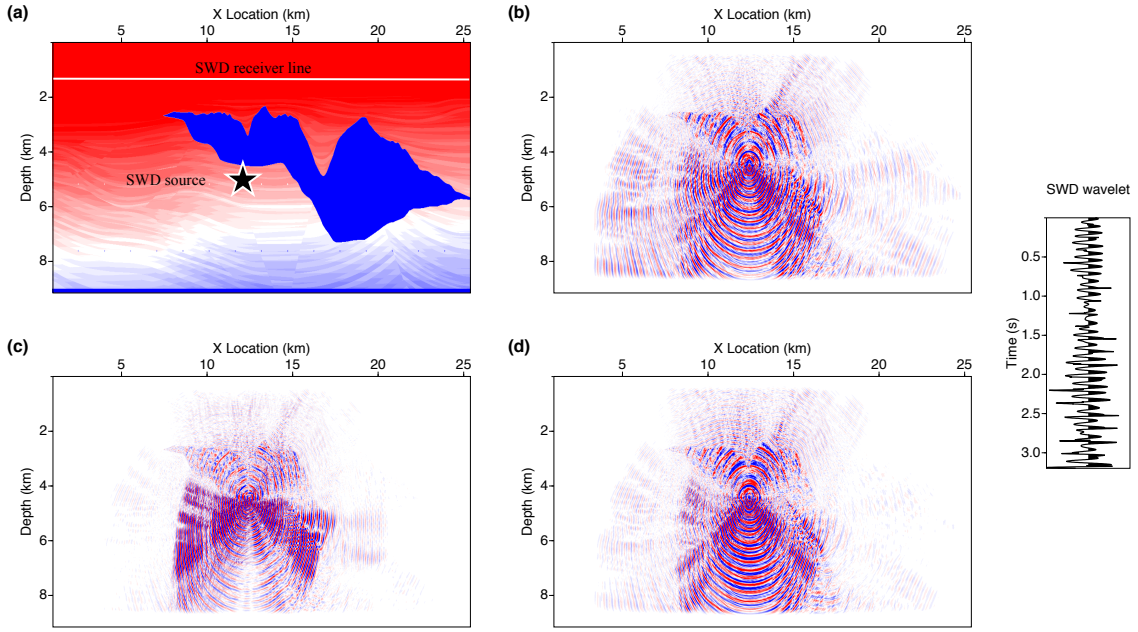

Figure 1: SWD wave simulation of Sigsbee model. a) Sigsbee primary velocity model. b) to d) Wavefield Shanpshots at T=3 (s) for Vertical, H1, and H2 components, respectively. SWD source signature is shown on the far right.

acquisition. The shear velocity model is generated by using $Vs = \frac{Vp}{\sqrt{3}}$. The average values of ε, δ, $\mathbf{Q}_{11}$, , $\mathbf{Q}_{13}$, $\mathbf{Q}_{33}$, $\mathbf{Q}_{55}$ are $0.2, 0.1, 50, 40, 30, 60$. Thomson parameters and Quality matrices follow the structure of the primary velocity. To simulate SWD data in this VTI viscoelastic media, we use a deviated well configuration and place the bit under the salt body. The black star in Figure 1a shows the location of the drill bit source. Then, we use equation (11) and simulate SWD source signature (shown in far right corner of Figure 1). Figures 1b to 1d show the snapshots of wavefield propagation after 3 seconds for the Vertical, H1 (XZ direction), and H2 components, respectively. The first observation is that in the case of SWD data, the source signature is correlative and non-impulsive. Thus, the wavefields are more complicated than impulsive sources. Another interesting observation is that the salt-body traps most of the energy of the source, and the recorded data on top of the salt body are weak. However, compared to surface seismic, the raypaths for SWD acquisition are shorter and they have different coverage. Thus, they provide a more meaningful signal than the conventional surface seismic acquisition. Figure 2 shows the 10-second recording of vertical, H1, and H2 components for the source-receiver geometry shown in Figure 1a. The simulated data has rich information in all components, which can add great value in subsurface imaging and inversion of such complex models.

Conclusions

We have derived a system of equations for simulating multicomponent SWD in viscoelastic media. We useed anisotropy in velocity and attenuation. Later, we implemented drill string dynamic modeling based on wave equation and top-drive hook-load and hook-speed measurements to simulate correlative and non-impulsive SWD source signature. We successfully tested the forward modeling engine on the Sigsbee model. Numerical examples showed the rich information on the multicomponent SWD data. This data can potentially reduce uncertainties in subsurface imaging and full-waveform inversion.

Acknowledgements

This work was supported by the University of Calgary's Canada First Research Excellence Fund Program, the Global Research Initiative in Sustainable Low Carbon Unconventional Resources.

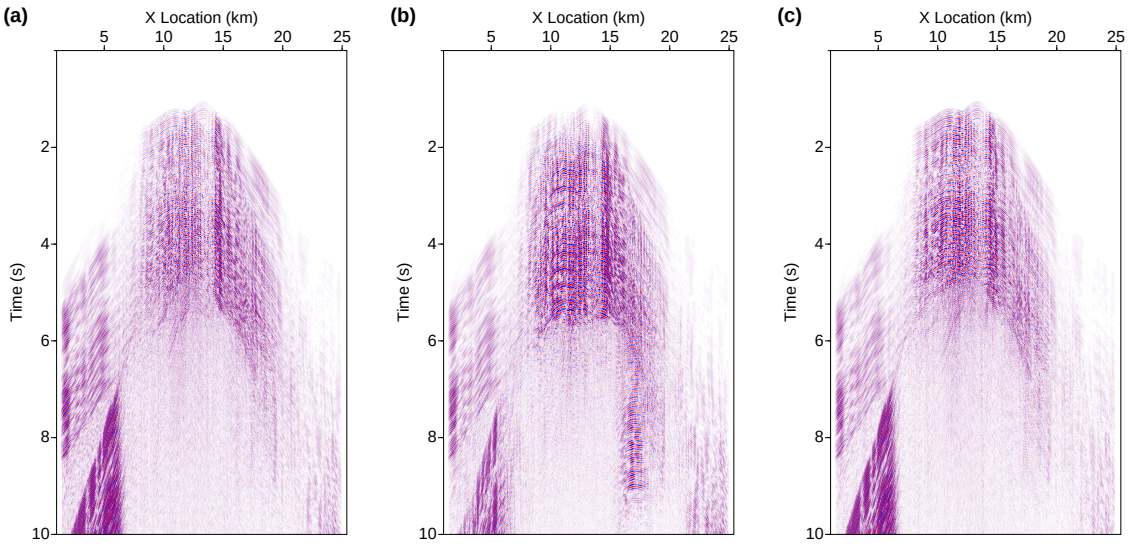

Figure 2: SWD data simulated using Sigsbee model. a) Vertical, b) H1, and c) is H2 components.

References

Auriol, J., Kazemi, N., Shor, R.J., Innanen, K.A. and Gates, I.D. [2019] A Sensing and Computational Framework for Estimating the Seismic Velocities of Rocks Interacting With the Drill Bit. *IEEE Transactions on Geoscience and Remote Sensing*.

Blanch, J.O., Robertsson, J.O. and Symes, W.W. [1993] Viscoelastic finite-difference modeling. In: *Expanded Abstracts*. 990–993.

Christensen, R. [1982] *Theory of Viscoelasticity, An Introduction*. Academic Press, New York.

Day, S.M. and Minster, J.B. [1984] Numerical simulation of attenuated wavefields using a Padé approximant method. *Geophysical Journal International*, **78**(1), 105–118.

Du, X., Fletcher, R.P. and Fowler, P.J. [2008] A new pseudo-acoustic wave equation for VTI medium. In: *Expanded Abstracts*. H033.

Duveneck, E. and Bakker, P.M. [2011] Stable P-wave modeling for reverse-time migration in tilted TI media. *Geophysics*, **76**(2), no. 2, S65–S75.

Fathalian, A., Trad, D.O. and Innanen, K.A. [2020] An approach for attenuation-compensating multidimensional constant-Q viscoacoustic reverse time migration. *Geophysics*, **85**(1), no. 1, S33–S46.

Fathalian, A., Trad, D.O. and Innanen, K.A. [2021] Q-compensated reverse time migration in tilted transversely isotropic media. *Geophysics*, **86**(1), S73–S89.

Kazemi, N., Auriol, J., Innanen, K., Shor, R. and Gates, I. [2020] Successive Full-waveform inversion of surface seismic and seismic-while-drilling datasets without low frequencies. In: *82nd EAGE Annual Conference & Exhibition*, 2020. European Association of Geoscientists & Engineers, 1–5.

Kazemi, N. and Sacchi, M.D. [2014] Sparse multichannel blind deconvolution. *Geophysics*, **79**(5), V143–V152.

Kazemi, N., Shor, R. and Innanen, K. [2018a] Illumination compensation with seismic-while-drilling plus surface seismic imaging. In: *80th EAGE Conference and Exhibition 2018*. 1–5.

Kazemi, N., Shor, R. and Innanen, K. [2018b] Imaging with a seismic-while-drilling dataset. *Proc. CSPG CSEG CWLS Conv*, 1–4.

Kjartansson, E. [1979] Constant Q-wave propagation and attenuation. *Journal of Geophysical Research: Solid Earth*, **84**(B9), 4737–4748.

Pipkin, A. [1986] *Lectures on Viscoelasticity Theory*. Springer.

Zhu, T. and Carcione, J.M. [2014] Theory and modelling of constant-Q P-and S-waves using fractional spatial derivatives. *Geophysical Journal International*, **196**(3), 1787–1795.